Vol. 41 — N° 2 06 17 p. 283 – 302

GEOSTANDARDS and GEOANALYTICAL RESEARCH

Mass-Independent and Mass-Dependent Ca Isotopic Compositions of Thirteen Geological Reference Materials Measured by Thermal Ionisation Mass Spectrometry

Yongsheng **He** (1)*, Yang **Wang** (1), Chuanwei **Zhu** (1), Shichun **Huang** (2) and Shuguang **Li** (1)

(1) State Key Laboratory of Geological Processes and Mineral Resources, School of Earth Sciences and Mineral Resources, China University of Geosciences, Beijing, 100083, China

(2) Department of Geoscience, University of Nevada, 4505 Maryland Parkway, Las Vegas, NV, 89154, USA

* Corresponding author. e-mail: heys@cugb.edu.cn

We report mass-independent and mass-dependent Ca isotopic compositions for thirteen geological reference materials, including carbonates (NIST SRM 915a and 915b), Atlantic seawater as well as ten rock reference materials ranging from peridotite to sandstone, using traditional ε and δ values relative to NIST SRM 915a, respectively. Isotope ratio determinations were conducted by independent unspiked and ^{43}Ca-^{48}Ca double-spiked measurements using a customised Triton Plus TIMS. The mean of twelve measurement results gave $\varepsilon^{40/44}$Ca values within ± 1.1, except for GSP-2 that had $\varepsilon^{40/44}$Ca = 4.04 ± 0.15 (2SE). Significant radiogenic ^{40}Ca enrichment was evident in some high K/Ca samples. At an uncertainty level of ± 0.6, all reference materials had the same $\varepsilon^{43/44}$Ca and $\varepsilon^{48/44}$Ca values. We suggest the use of $\delta^{44/42}$Ca to report mass-dependent Ca isotopic compositions. The precision under intermediate measurement conditions for $\delta^{44/42}$Ca over eight months in our laboratory was ± 0.03‰ (with $n \geq 8$ repeat measurements). Measured igneous reference materials gave $\delta^{44/42}$Ca values ranging from 0.27‰ to 0.54‰. Significant Ca isotope fractionation may occur during magmatic and metasomatism processes. Studied reference materials with higher (Dy_n/Yb_n) tend to have lower $\delta^{44/42}$Ca, implying a potential role of garnet in producing magmas with low $\delta^{44/42}$Ca. Sandstone GBW07106 had a $\delta^{44/42}$Ca value of 0.22‰, lower than all igneous rocks studied so far.

Keywords: mass-dependent fractionation, mass-independent fractionation, Ca isotopes, double-spike method, geological reference materials, igneous processes.

Received 13 Jun 16 – Accepted 11 Oct 16

Calcium is a major element on the Earth and plays an essential role in geological and biological processes. It has six stable isotopes: ^{40}Ca, ^{42}Ca, ^{43}Ca, ^{44}Ca, ^{46}Ca and ^{48}Ca. Variations in Ca isotopic ratios can be caused by nucleosynthetic anomaly, the decay of ^{40}K to ^{40}Ca and mass-dependent isotope fractionation. Calcium isotopic variations thus may provide important constraints on the origin and evolution of planets (Simon *et al.* 2009, Huang *et al.* 2012), age information by the ^{40}K-^{40}Ca isotopic system (Marshall and DePaolo 1982, 1989, Caro *et al.* 2010) and the global Ca cycle from the surface to deep mantle (De La Rocha and DePaolo 2000, Farkaš *et al.* 2007, 2011, Huang *et al.* 2011, Zhu *et al.* 2015). The reported $\delta^{44/42}$Ca variation in terrestrial samples is about 2.0‰ (Fantle and Tipper 2014), and thus, precise and accurate Ca isotopic measurement is essential for the use of calcium isotopes as geochemical tools.

Difficulties in obtaining high-precision Ca isotopic data include the large natural abundance difference, the large relative mass range, asymmetrical peak shapes, strong isobaric interferences in multi-collector-inductively coupled plasma-mass spectrometry (MC-ICP-MS), nonideal evaporation and ionisation processes in thermal ionisation mass spectrometry (TIMS) and degradation of Faraday cups (Heuser *et al.* 2002, Fantle and Bullen 2009, Boulyga 2010, Holmden and Bélanger 2010, Morgan *et al.* 2011, Lehn *et al.* 2013, Fantle and Tipper 2014, Zhu *et al.* 2016). Typical intermediate measurement precision for $\delta^{44/40}$Ca is ~ 0.1‰ (Tipper *et al.* 2006, Huang *et al.* 2010, Lehn *et al.* 2013, Valdes *et al.* 2014, Zhu *et al.* 2016).

doi: 10.1111/ggr.12153

Here, we report (a) new analytical developments for Ca isotopic measurement at the Isotope Geochemistry Laboratory (State Key Laboratory of Geological Processes and Mineral Resources, China University of Geosciences, Beijing) and (b) the characterisation of Ca isotopic compositions of thirteen geological reference materials. These include commonly used carbonate reference materials (NIST SRM 915a and 915b), Atlantic seawater, as well as ten rock reference materials ranging in type from peridotite to sandstone.

Two types of Ca isotopic effects

Natural Ca isotopic effects can be divided into two types, namely mass-independent and mass-dependent isotopic effects (e.g., Niederer and Papanastassiou 1984, Huang *et al.* 2012). During unspiked measurements, natural and instrumental mass-dependent fractionation is internally corrected to $^{42}Ca/^{44}Ca = 0.31221$ using the exponential law (Russell *et al.* 1978, Hart and Zindler 1989); consequently, mass-independent Ca isotopic data describe radiogenic ^{40}Ca excess due to ^{40}K decay and addition of nucleosynthetic components with nonsolar isotopic compositions. Mass-independent Ca isotopic data are commonly reported in traditional ε values relative to a certain geological reservoir, for example, carbonate NIST SRM 915a (Huang *et al.* 2012, Naumenko-Dèzes *et al.* 2015).

$$\varepsilon^{i/44}\mathrm{Ca(SAM)} = \left[\frac{\left(^{i}\mathrm{Ca}/^{44}\mathrm{Ca_{SAM}}\right)_{\mathrm{N}}}{\left(^{i}\mathrm{Ca}/^{44}\mathrm{Ca_{SRM915a}}\right)_{\mathrm{N}}} - 1\right] \times 1000 \quad (1)$$

where *i* can be 40, 43, 46 or 48, and subscript N represents internal normalisation to $^{42}Ca/^{44}Ca = 0.31221$.

Mass-dependent (stable) isotopic data describe the natural isotopic variations intrinsic to the samples that occur due to atomic mass difference among isotopes. Therefore, only instrumental fractionation is corrected using the double-spike technique with TIMS (Heuser *et al.* 2002, Huang *et al.* 2010, Lehn *et al.* 2013, Zhu *et al.* 2016) and the calibrator-sample bracketing method with MC-ICP-MS (Tipper *et al.* 2006, Valdes *et al.* 2014). Mass-dependent isotopic data are reported as $\delta^{44/40}Ca$ or $\delta^{44/42}Ca$:

$$\delta^{44/i}\mathrm{Ca(SAM)} = \left(\frac{^{44}\mathrm{Ca}/^{i}\mathrm{Ca_{SAM}}}{^{44}\mathrm{Ca}/^{i}\mathrm{Ca_{SRM915a}}} - 1\right) \times 1000 \quad (2)$$

where *i* can be 40 or 42. It should be noted that $\delta^{44/40}Ca$ includes contributions both from mass-dependent isotope fractionation and from the decay of ^{40}K. The radiogenic excess of ^{40}Ca relative to NIST SRM 915a can be calculated from the measured $\delta^{44/40}Ca$ and $\delta^{44/42}Ca$ based on the following expression (Farkaš *et al.* 2011):

$$\varepsilon^{40/44}\mathrm{Ca} = \left[\left(\delta^{44/42}\mathrm{Ca} \times 2.0483\right) - \delta^{44/40}\mathrm{Ca}\right] \times 10 \quad (3)$$

where the coefficient of 2.0483 represents the slope of the mass-dependent fractionation between $\delta^{44/40}Ca$ and $\delta^{44/42}Ca$ following the exponential law (Farkaš *et al.* 2011, Huang *et al.* 2012).

Published studies and associated problems

The entire $\delta^{44/42}Ca$ range of terrestrial samples is about 2.0‰, and thus, the use of Ca isotopes as a proxy requires precise and accurate measurement (Fantle and Tipper 2014). Currently, stable Ca isotopic ratios can be measured with an intermediate precision ('external precision') of ± 0.10‰ on the $\delta^{44/40}Ca$ scale by TIMS and by MC-ICP-MS (Tipper *et al.* 2006, Huang *et al.* 2010, Lehn *et al.* 2013, Valdes *et al.* 2014, Zhu *et al.* 2015, 2016). Comparison of stable Ca isotopic data from different laboratories is complicated, because the commonly used $\delta^{44/40}Ca$ reflects the combined effect of radiogenic ^{40}Ca enrichment and mass-dependent fractionation (Fantle and Tipper 2014). Discrimination of these two types of effects can be obtained using combined mass-independent and mass-dependent isotopic measurements (Huang *et al.* 2012, Schiller *et al.* 2012) or based on simultaneously reported $\delta^{44/40}Ca$ and $\delta^{44/42}Ca$ using a ^{43}Ca-^{48}Ca double-spike (Huang *et al.* 2010, Farkaš *et al.* 2011). However, these combined data have been rarely reported in the literature. For interlaboratory comparison purposes, it is necessary to better characterise both mass-independent and mass-dependent Ca isotopic compositions of geological reference materials.

It remains difficult to compare directly mass-independent Ca isotopic ratios obtained by different laboratories. Published $(^{40}Ca/^{44}Ca)_N$ of NIST SRM 915a ranges from 46.106 to 47.1649 (Naumenko-Dèzes *et al.* 2015 and references therein). Naumenko-Dèzes *et al.* (2015) report internally consistent Ca isotopic ratios for NIST SRM 915a and 915b using a customised Triton Plus TIMS instrument that allowed simultaneous measurement of ^{40}Ca to ^{48}Ca. An improved exponential law using two stable isotopic ratio pairs (e.g., $^{42}Ca/^{44}Ca$ and $^{48}Ca/^{44}Ca$) has been shown to properly correct the instrumental mass bias, and argued to work for natural samples (Naumenko-Dèzes *et al.* 2015). It is necessary to check whether these absolute values can be reproduced in other laboratories.

Measurement procedure

Chemistry procedures

Typically, sample powders weighing 3–50 mg were dissolved in a mixture of 1.5 ml concentrated HF and 0.5 ml concentrated HNO_3 in 6-ml Teflon™ beakers at 100 °C for three days. The sample solutions were then dried down and evaporated with 0.5 ml concentrated HCl at 120 °C three times. The products were finally dissolved in 0.5 ml 2.5 mol l^{-1} HCl. For mass-independent isotopic measurement, an aliquot of each sample solution containing *ca.* 50 μg Ca was evaporated to dryness, and re-dissolved in 50 μl 2.5 mol l^{-1} HCl for column chemistry. For mass-dependent isotopic measurement, an aliquot of each sample solution containing *ca.* 50 μg Ca was mixed with an appropriate amount of ^{43}Ca-^{48}Ca double-spike solution (Table 1) so that the $^{48}Ca/^{40}Ca$ ratio of the mixture was *ca.* 0.1145. The spiked samples were then homogenised by refluxing at 120 °C overnight, evaporated to dryness again and dissolved in 50 μl 2.5 mol l^{-1} HCl. Calcium was purified using quartz columns (3 mm in diameter and *ca.* 11 cm in length) filled with AG50W-X12 (200–400 mesh; Bio-Rad, Hercules, CA, USA) resin. Columns were precleaned and conditioned with 10 ml 6 mol l^{-1} HCl, 5 ml high-purity water and 2 ml 2.5 mol l^{-1} HCl in a stepwise fashion. Sample solutions with ~ 50 μg Ca were loaded using 50 μl 2.5 mol l^{-1} HCl. Matrix elements (e.g., Fe, Mg, Ti, K and Al) were removed by 5 ml 2.5 mol l^{-1} HCl, and Ca was collected using 3.5 ml 2.5 mol l^{-1} HCl without collecting significant amount of Sr (Figure 1). Each sample was passed through the column twice. The Ca yield after two-column chemistry was about 90%. The purified Ca was then evaporated to dryness with several drops of concentrated HNO_3 for isotopic measurement. Double-distilled acids were used, and the whole procedure Ca blank typically ranged from 13 to 58 ng, which is < 0.2% of the processed samples.

Mass spectrometry

The Triton Plus TIMS at the Isotope Geochemistry Lab was equipped with a customised Faraday cup (L5) for ^{40}Ca and a Faraday cup (H4) for ^{48}Ca, allowing static measurement of masses from 40 to 48 amu. All Faraday cups were connected to 10^{11} Ω resistors. All Ca isotopes and ^{41}K were routinely collected in one single cup configuration line as shown in Figure 2. Calcium isotopes were typically measured with a total intensity of 100–300 pA, which yielded a ^{40}Ca signal of *ca.* 8–30 V. An optional second configuration line for ^{42}Ca and ^{44}Ca at the L3 and central Faraday cups, respectively, was added after 7 December 2015 to check whether the intermediate measurement precision was dominated by the low ^{42}Ca signal (typically ~ 100 mV). The isobaric interference of ^{40}K on ^{40}Ca was generally < 6 ppm and did not require correction.

A double-zone-refined Re filament assemblage was used for Ca isotopic measurements. After welding, filaments were degassed under vacuum for 10 min at 3.5 A, 20 min at 4.5 A and 30 s at 3.0 A with subsequent oxidising at room temperature for at least three days. About 5 μg Ca was loaded on the evaporation filament using 1 μl 3% HNO_3. The solution was slowly evaporated at a filament current of 0.5 A, then heated at 1.5 A for 1 min and finally heated up to dull red for 30 s (Huang *et al.* 2010). The loading blank was < 100 pg.

The Triton Plus TIMS sample wheel could host twenty-one filament assemblages. A typical measurement session

Table 1.
Internally normalised isotopic composition for NIST SRM 915a and ^{43}Ca-^{48}Ca double-spike (DS)

Samples	SRM 915a	DS (meas.)	DS (calib.)
$^{40}Ca/^{44}Ca$	47.1516(6)	3.57458(2)	3.57534(4)
$^{42}Ca/^{44}Ca$	0.31221	0.172803(2)	0.172821(1)
$^{43}Ca/^{44}Ca$	0.0648681(11)	15.9830(2)	15.9838(1)
$^{46}Ca/^{44}Ca$	0.0015125(19)	0.00045859	0.000446(1)
$^{48}Ca/^{44}Ca$	0.0886516(28)	32.0444(3)	32.0382(4)

Isotopic composition of NIST SRM 915a is given by a long-term mean of 237 times measurement over nine months (Table S1). Double-spike composition was first measured independently for four times (5 μg per load) and then calibrated for the remaining unresolved mass bias using double-spiked NIST SRM 915a data. The details are referred to the main text and Appendix S1. The errors are two times the standard error of the mean and correspond to the last figures shown.

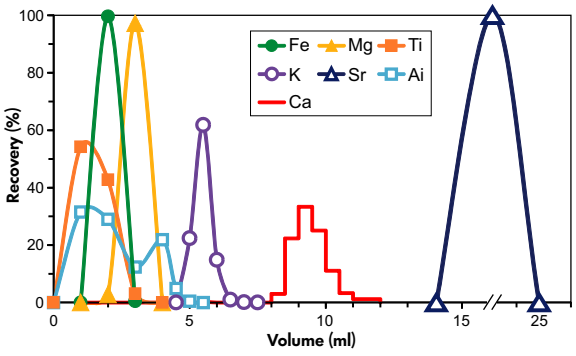

Figure 1. The Ca elution curve of BHVO-2 passed through columns (0.3 cm × 11 cm) filled with AG50W-X12 (200 to 400 mesh). [Colour figure can be viewed at wileyonlinelibrary.com]

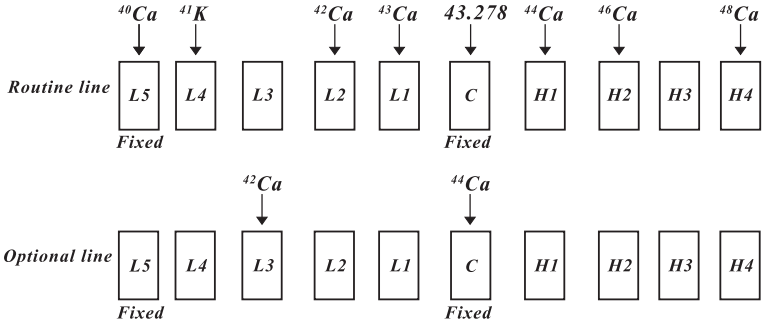

Figure 2. The Faraday cup configuration and amplifiers employed for the current study. A customised Faraday cup alignment allows simultaneous measurement of masses from 40 to 48 amu. An optional second configuration line for ^{42}Ca and ^{44}Ca at the L3 and central Faraday cups was adopted after 7 December 2015 to check whether the intermediate measurement precision was dominated by the low ^{42}Ca signal.

involved up to twenty-one filament assemblages hosted in a single wheel, which typically contained 2–3 NIST SRM 915a, 1–2 Atlantic Seawater or NIST SRM 915b and 16–18 unknown samples. During a measurement routine, the ion and evaporation filaments were heated up automatically. The ion filament was rapidly heated to 2500 mA in 3 min, and then, the evaporation filament was heated to 50 mA in 1 min. The ion and evaporation filaments were then heated up by increments of 50 mA and 30 mA alternately with a slope of 30 mA min^{-1} until a stable ^{40}Ca signal ranging from 10 to 30 V was obtained. Evaporation filament current was kept below 800 mA, which was important to obtain a stable instrumental mass bias. During the heating routine, ^{44}Ca was monitored for ion intensity. Source lenses were focused when ^{44}Ca reached 5 mV and then at the end of the heating routine. A routine measurement consisted of a peak centre on ^{44}Ca at H1 at the beginning and every eight blocks of data acquisition. Each block included a 60-s baseline measurement and fifteen cycles with an integration time of 16.776 s. Amplifier rotation for every block was enabled. Total analytical time was *ca.* 90 min for one filament assemblage, including a 30-min heating routine. Typically, each sample was loaded on three to four filaments, and each filament assemblage was measured two to three times, independently, from heating up to data acquisition. Mass-independent Ca isotopic data were internally corrected to ^{42}Ca/^{44}Ca = 0.31221 and reported in conventional ε values. For the mass-dependent isotopic effect, isotope fractionation in the laboratory, including low column chemistry yield and isotopic fractionation on TIMS, was corrected by a ^{43}Ca-^{48}Ca double-spike technique (Table 1). ^{42}Ca/^{44}Ca, ^{43}Ca/^{44}Ca and ^{48}Ca/^{44}Ca were used for double-spike data deduction with a procedure modified from Johnson and Beard (1999), Rudge *et al.* (2009) and Li *et al.* (2011), which is detailed in Appendix S1. Mass-dependent isotopic compositions of geological reference materials are reported in $\delta^{44/42}$Ca values after Farkaš *et al.* (2011).

Double-spike calibration

The ^{43}Ca-^{48}Ca double-spike was prepared by mixing ^{43}Ca and ^{48}Ca single spikes obtained from the Oak Ridge National Laboratory (USA) according to the optimised proportion predicted by Rudge *et al.* (2009). Its isotopic composition was then measured by four runs independently prepared from loading (5 µg of each filament) to data acquisition. The instrumental mass bias was preliminarily corrected to ^{43}Ca/^{48}Ca = 0.49878, obtained by a gravimetric method using the certificate values for single spikes, using the exponential law. As shown in Figure 3, linear correlations were found among the measured $(^{43}Ca/^{40}Ca)_N$, $(^{48}Ca/^{40}Ca)_N$ and $(^{44}Ca/^{40}Ca)_N$ values, after normalisation to ^{43}Ca/^{48}Ca = 0.49878, which reflect mixtures of double-spike and blank Ca during the sample loading procedure. The loading blank was then estimated to be < 100 pg. The run with the highest $(^{43}Ca/^{40}Ca)_N$ and $(^{48}Ca/^{40}Ca)_N$ represents the least contaminated double-spike, which was used to calculate the double-spike isotopic composition (Table 1). These measured isotopic ratios differ from the 'true' values because the instrumental mass bias was corrected to ^{43}Ca/^{48}Ca = 0.49878 with a large uncertainty. This ^{43}Ca/^{48}Ca normalisation value was obtained using a gravimetric method by weighing several milligrams of ^{43}Ca and ^{48}Ca single spikes during double-spike solution preparation. The double-spike composition was further calibrated based on 186 spiked NIST SRM 915a runs during May 2015 to September 2015 using a procedure detailed in Appendix S1, which makes a correction on ^{43}Ca/^{48}Ca by ~ 0.25‰. The NIST SRM 915a-calibrated ^{43}Ca-^{48}Ca double-spike composition is reported in Table 1. Using these calibrated values, 100

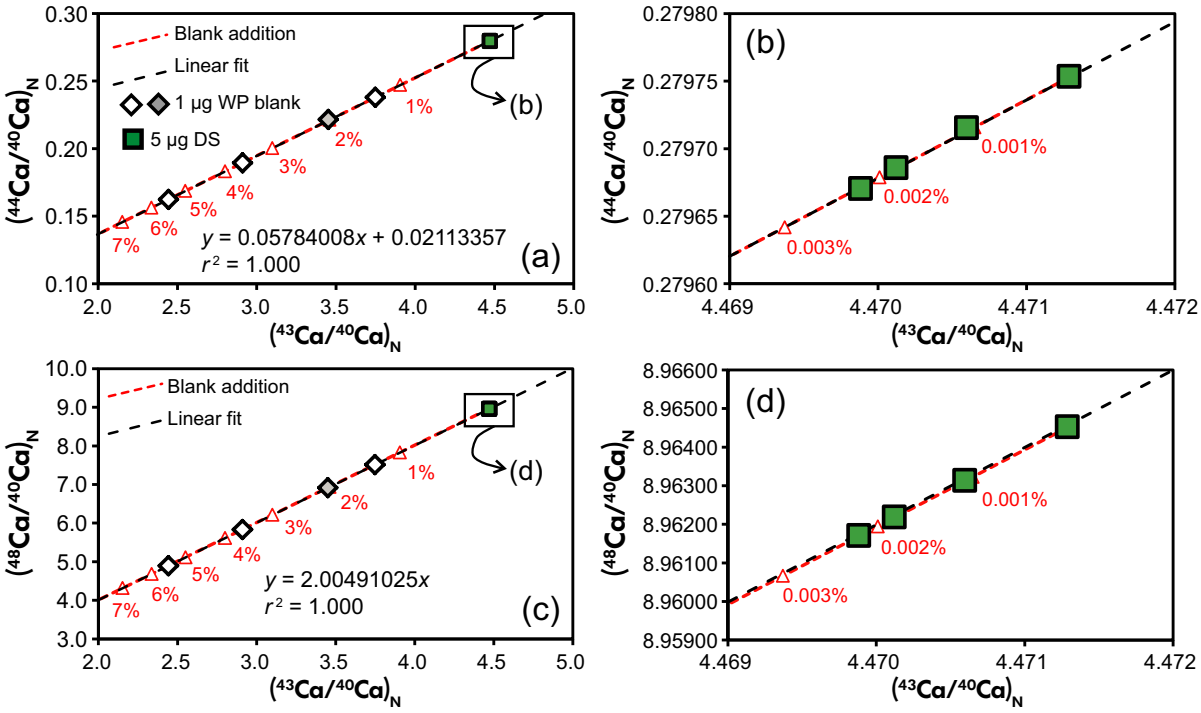

Figure 3. Determination of the isotopic composition of the double-spike by blank subtraction: (a) $(^{44}Ca/^{40}Ca)_N$ vs. $(^{43}Ca/^{40}Ca)_N$ diagram, (b) inset to Figure 3a, (c) $(^{48}Ca/^{40}Ca)_N$ vs. $(^{43}Ca/^{40}Ca)_N$ diagram and (d) inset to Figure 3c. Mass bias was normalised against $^{43}Ca/^{48}Ca$ = 0.49878. Linear fitting was conducted for four runs on the double-spike independent from loading (5 µg each, green filled squares) to data acquisition and three runs of whole procedure blank (traced by 1 µg double-spike each, unfilled diamonds) prior to September 2015. The whole procedure blank measured on 29 November 2015 (grey filled diamond) was not used for linear fitting, but is also plotted here for comparison. Measurement repeatability uncertainties are below the size of symbols. [Colour figure can be viewed at wileyonlinelibrary.com]

independent runs of spiked NIST SRM 915a from October 2015 to December 2015 yielded mean $\delta^{44/40}Ca$ and $\delta^{44/42}Ca$ values of 0.00 ± 0.12‰ (2*s*) and -0.03 ± 0.08‰ (2*s*), respectively. The slight shift in mean $\delta^{44/42}Ca$ may be attributed to drift in the H4 Faraday cup efficiency when aging, and thus, all $\delta^{44/42}Ca$ data obtained after 25 September 2015 were re-normalised by subtracting -0.03 accordingly.

Effect of heterogeneous evaporation: A Monte Carlo approach

During Ca isotopic measurement, the intermediate precision is always worse than the measurement repeatability ('internal precision') (Heuser *et al.* 2002, Fantle and Bullen 2009, Lehn *et al.* 2013, Lehn and Jacobson 2015, Naumenko-Dèzes *et al.* 2015). This is also true for our measurements of NIST SRM 915a: the intermediate precision was two to eight times of that of measurement repeatability for single mass-independent and mass-dependent Ca isotopic measurements. For example, the two standard deviation value of $\delta^{44/40}Ca$ was 0.16‰, compared with the mean measurement repeatability of 0.02‰ (Tables S1 and S3). During TIMS measurement, non-ideal evaporation and ionisation processes have been proposed as a major reason for the worse intermediate precisions observed (Fantle and Bullen 2009, Fantle and Tipper 2014, Lehn and Jacobson 2015). Sample Ca loaded on the Re or Ta filament is not an ideal point source (Fantle and Bullen 2009, Lehn and Jacobson 2015, Naumenko-Dèzes *et al.* 2015), and mixing of signals from independent evaporation sources can lead to the violation of the commonly adopted exponential law, which leads to erroneous data (Figure 4a; Fantle and Bullen 2009, Lehn and Jacobson 2015). The phenomenon is referred to as heterogeneous evaporation (HE) effect after Fantle and Bullen (2009). We used a Monte Carlo approach to evaluate this effect and to test how it can be corrected for. In this approach, Ca with an isotopic composition identical to NIST SRM 915a (Table 1) was to evaporate from *n* (2 to 20) independent sources on a filament, and each followed the exponential law. The fractionation factor

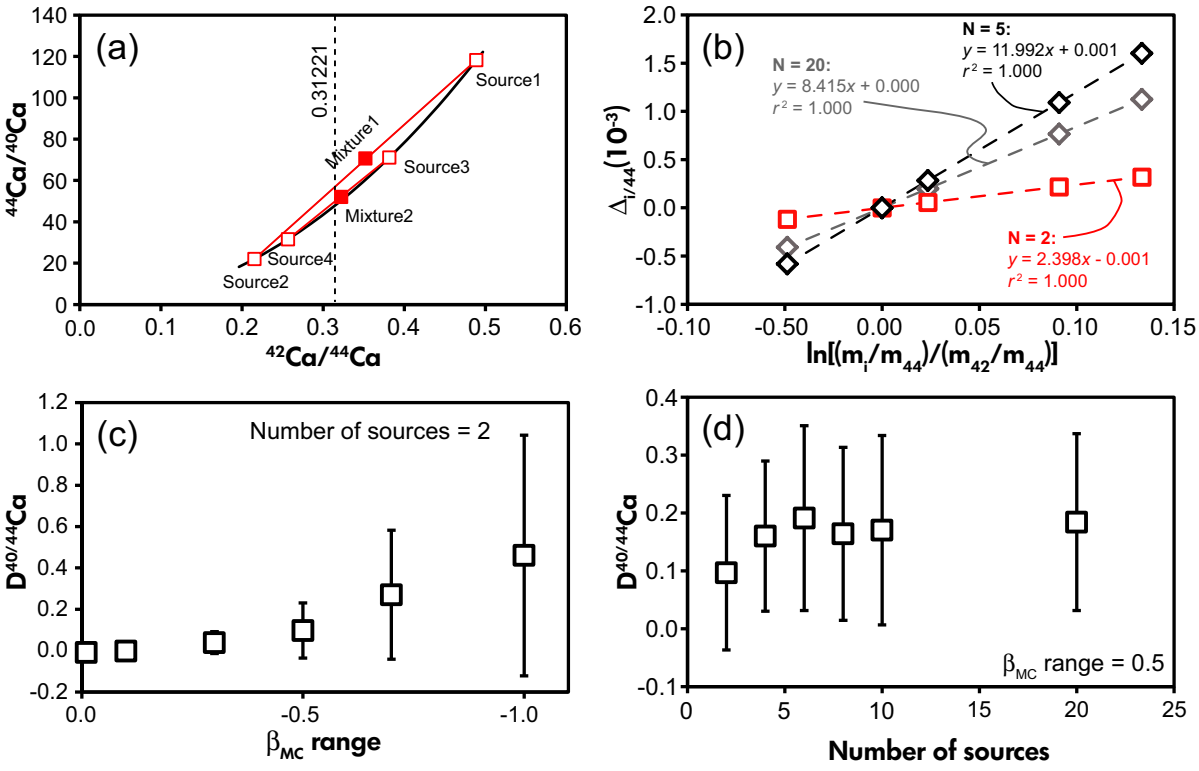

Figure 4. Simulation of the heterogeneous evaporation effect using a Monte Carlo approach. A cartoon shown mixing processes of multiple sources and regression of data to $^{42}Ca/^{44}Ca$ = 0.31221 based on the exponential law (a). The simulation approach was detailed in the main text. $\Delta_{i/44}$, where *i* can be 40, 42, 43, 46 and 48, was calculated by the difference between the theoretically measured ratios and the true values following a formula of the exponential law (Equations 13 and 14 in Appendix S1). As shown in (b), $\Delta_{i/44}$ varies with the isotopic ratio pair mass dependently. Difference from the measured $(^{40}Ca/^{44}Ca)_N$ and the true value was expressed as a D value ($D = \left[\frac{(^{40}Ca/^{44}Ca)_N}{(^{40}Ca/^{44}Ca)_T} - 1\right] \times 10^4$). The mean D values were plotted against the β_{MC} range and number of independent evaporation sources (c and d), with error bars representing two standard deviation. [Colour figure can be viewed at wileyonlinelibrary.com]

$$\beta_{MC} = \ln\left(\frac{(^{i}Ca/^{44}Ca)_M}{(^{i}Ca/^{44}Ca)_T}\right) / \ln\left(\frac{m_i}{m_{44}}\right) \quad (4)$$

$$D = \left[\frac{(^{i}Ca/^{44}Ca)_N}{(^{i}Ca/^{44}Ca)_T} - 1\right] \times 10^4 \quad (5)$$

where *i* can be 40, 42, 43, 46 or 48, and M and T represent the measured and true ratios, respectively, of each source was randomly set between 0 and an arbitrary value (β_{MC} range, e.g., 0.01, 0.1, 0.3, 0.5, 0.7, 1.0). Contribution to the total signal from each source was also randomly set. Isotopic ratios were then calculated using the accumulated signals from all independent sources, and corrected to $^{42}Ca/^{44}Ca$ = 0.31221 using the exponential law. During our Monte Carlo approach, 100 cases were simulated for each pair of N and β_{MC}. Simulations reveal that after internal normalisation to $^{42}Ca/^{44}Ca$ = 0.31221, $(^{40}Ca/^{44}Ca)_N$ ratios were erroneously higher than the true value due to the HE effect. Their deviations were measured as D, defined as:

This increased with increasing β_{MC} range that measures β_{MC} difference among independent evaporation sources, and was not correlated with the number of evaporating sources (Figure 4). The β_{MC} values during our Ca isotopic analyses were fairly constant at -0.17 ± 0.02 (2*s*, *n* = 987/988), except for one run that yielded a β_{MC} of -0.11 and was treated as an outlier. In addition, the β_{MC} value in each individual run did not change significantly with time. Therefore, the error introduced by the HE effect for Ca isotopic analyses was estimated to be < 10 ppm, which is negligible. Additional sources of uncertainty must account for the larger intermediate precision and will be discussed in the next section.

The Monte Carlo simulations also reveal that the extent of deviation from the exponential law due to the HE effect is mass-dependent, which can be expressed following a formula of the exponential law:

$$\Delta_{\frac{i}{44}} = \ln\left(\frac{\left({}^{i}\mathrm{Ca}/{}^{44}\mathrm{Ca}\right)_{\mathrm{N}}}{\left({}^{i}\mathrm{Ca}/{}^{44}\mathrm{Ca}\right)_{\mathrm{T}}}\right) / \ln\left(\frac{m_i}{m_{44}}\right) \quad (6)$$

where i can be 40, 42, 43, 46 and 48 and m refers to the atomic masses. Our simulations thus provide a theoretical explanation for the concept that the HE effect during mass-dependent Ca isotopic measurement can be optimised by choosing double-spike pairs based on an 'average mass rule' (Lehn and Jacobson 2015). The 'average mass rule' predicts a minimised HE effect when the average mass of a double-spike is close to that of the normalising ratio (e.g., using ^{42}Ca-^{43}Ca double-spike to monitor ^{44}Ca/^{40}Ca). It is interesting to note that $\Delta_{i/44}$ and $\ln[(m_i/m_{44})/(m_{42}/m_{44})]$ rigorously follow a linear trend crossing the origin (Figure 4b). This validates a secondary correction using a second stable isotopic ratio other than ^{42}Ca/^{44}Ca = 0.31221 to correct the HE effect for mass-independent isotopic measurement (see Appendix S1 for details):

$$\frac{\left({}^{x}\mathrm{Ca}/{}^{44}\mathrm{Ca}\right)_{\mathrm{N}}}{\left({}^{x}\mathrm{Ca}/{}^{44}\mathrm{Ca}\right)_{\mathrm{T}}} = \left[\frac{\left({}^{y}\mathrm{Ca}/{}^{44}\mathrm{Ca}\right)_{\mathrm{N}}}{\left({}^{y}\mathrm{Ca}/{}^{44}\mathrm{Ca}\right)_{\mathrm{T}}}\right]^{A} \quad (7)$$

where

$$A = \frac{\ln\left(\frac{m_x}{m_{42}}\right) \times \ln\left(\frac{m_x}{m_{44}}\right)}{\ln\left(\frac{m_y}{m_{42}}\right) \times \ln\left(\frac{m_y}{m_{44}}\right)} \quad (8)$$

^{y}Ca/^{44}Ca is the stable isotopic ratio for secondary correction and could be ^{43}Ca/^{44}Ca or ^{48}Ca/^{44}Ca. Subscript N and T represent the corrected ratios against ^{42}Ca/^{44}Ca = 0.31221 and the supposed true values, respectively. As shown in Figure S1, even theoretical runs with significant HE effect can be properly corrected by the above formula. A similar formula has been proposed for high-precision ^{142}Nd isotopic measurement (Caro *et al.* 2003) and also used for Ca isotopic measurement (Naumenko-Dèzes *et al.* 2015). Given that deduction of the secondary correction is only based on the exponential law and a mixing model, this secondary correction could be applicable for high-precision isotopic measurement for other radiogenic isotopes with at least two stable isotopic ratio pairs to correct for possible HE effect. Specifically, this secondary correction was not adopted for the mass-independent Ca isotopic data reported in this study, because HE effect is negligible and time-dependent drift in the measured $(^{48}\mathrm{Ca}/^{44}\mathrm{Ca})_{\mathrm{N}}$ that will discussed below may cause additional errors.

Mass-independent isotopic compositions of geological materials

Time-dependent drift of Faraday cup efficiency

During seventeen analytical sessions, 256 unspiked NIST SRM 915a measurements were carried out to monitor possible Faraday cup efficiency drift and the intermediate measurement precision (over 9 months) of mass-independent Ca isotopic determinations (Figure 5 and Table S1). Nineteen out of 256 runs, identified by $(^{40}\mathrm{Ca}/^{44}\mathrm{Ca})_{\mathrm{N}}$ < median - (maximum - median), yield $(^{40}\mathrm{Ca}/^{44}\mathrm{Ca})_{\mathrm{N}}$ substantially lower than average and were treated as outliers (Figure 5a). Contamination of spikes from the ion sources, possibly due to spiked analytical sessions that were measured alternately with unspiked ones, can be ruled out by the measured $(^{43}\mathrm{Ca}/^{44}\mathrm{Ca})_{\mathrm{N}}$ and $(^{48}\mathrm{Ca}/^{44}\mathrm{Ca})_{\mathrm{N}}$ ratios of these outliers comparable to the majority data (Figure 5a and Table S1). Several parameters have been proposed that affect the accuracy of Ca isotopic determinations, including Faraday cup efficiency drift (Simon *et al.* 2009, Caro *et al.* 2010, Holmden and Bélanger 2010, Lehn *et al.* 2013), heterogeneous evaporation effect (Hart and Zindler 1989, Fantle and Bullen 2009) and ion optical aberrations (Fletcher *et al.* 1997, Holmden and Bélanger 2010). No systematic drift on the measured $(^{40}\mathrm{Ca}/^{44}\mathrm{Ca})_{\mathrm{N}}$ was evident between March 2015 and December 2015. The width of the graphite insert for the Faraday cup L5 was doubled and customised for the most intense signal (^{40}Ca). This study thus confirms that the customised L5 cup is immune to efficiency drift (Naumenko-Dèzes *et al.* 2015). In addition, the heterogeneous evaporation effect leads to measured $(^{40}\mathrm{Ca}/^{44}\mathrm{Ca})_{\mathrm{N}}$ higher than the true value (Figure 4a and section 'Effect of heterogeneous evaporation'), and thus, it cannot account for the low $(^{40}\mathrm{Ca}/^{44}\mathrm{Ca})_{\mathrm{N}}$ values (Figure 5a). The low $(^{40}\mathrm{Ca}/^{44}\mathrm{Ca})_{\mathrm{N}}$ of the outlier runs can be explained by selective loss of the ^{40}Ca ion collected in the low mass edge Faraday cup, but without any effect on other isotopic ratios. The only explanation of this phenomenon is clipping on ^{40}Ca after ion-beam dispersion, for example, interaction with the metal mask in front of the L5 cup, which is used to keep the peak shape of ^{40}Ca same to other masses.

No $(^{43}\mathrm{Ca}/^{44}\mathrm{Ca})_{\mathrm{N}}$ drift was observed for NIST SRM 915a, but a systematic drift was evident for $(^{48}\mathrm{Ca}/^{44}\mathrm{Ca})_{\mathrm{N}}$ (Figure 5c, d). In detail, measured $(^{48}\mathrm{Ca}/^{44}\mathrm{Ca})_{\mathrm{N}}$ gradually decreased from 0.088675 ± 29 (2*s*, *n* = 66) between March 7 and March 16, 0.088655 ± 36 (2*s*, *n* = 65) between April 16 and July 7, to 0.088635 ± 20 (2*s*, *n* = 106) between July 9 and December 30. This may reflect a drift in the H4 Faraday cup efficiency, possibly due to the

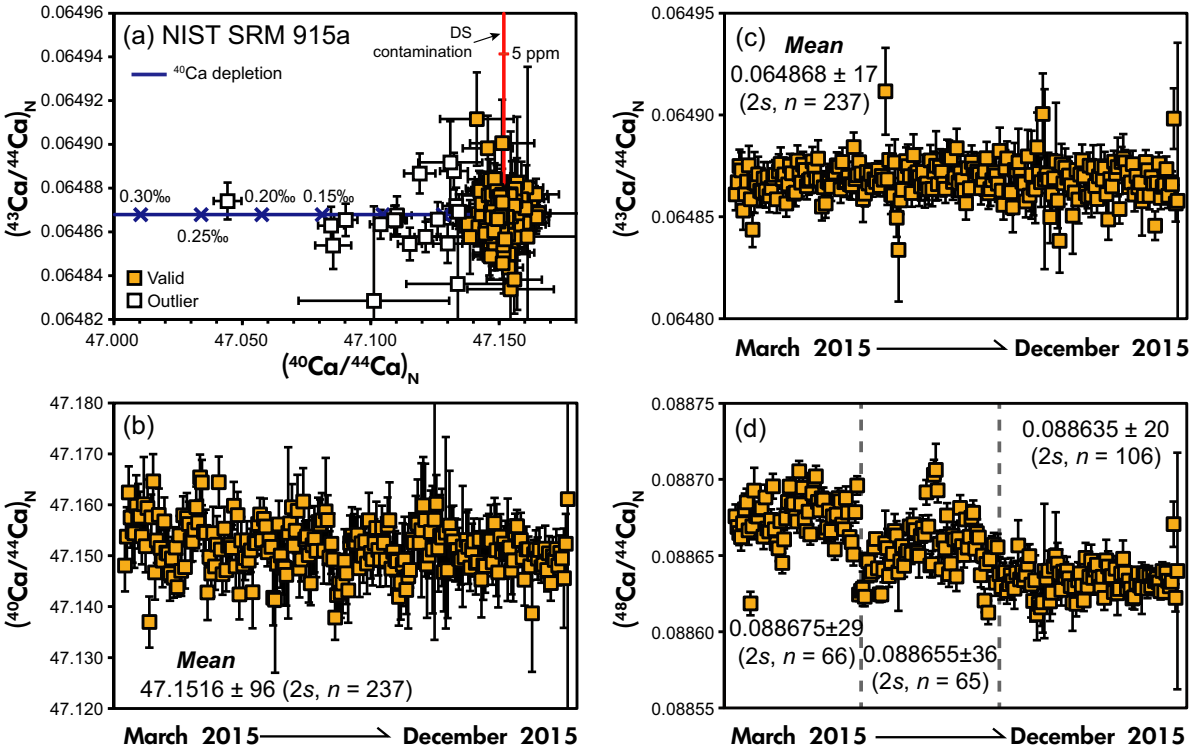

Figure 5. Mass-independent isotopic ratios for NIST SRM 915a measured from March 2015 to December 2015. All data are internally normalised to $^{42}Ca/^{44}Ca$ = 0.31221 (Russell *et al.* 1978) assuming the exponential law. Nineteen out of 256 runs, identified by $(^{40}Ca/^{44}Ca)_N$ < median - (maximum - median), yield $(^{40}Ca/^{44}Ca)_N$ substantially lower than average and were treated as outliers (unfilled squares in (a)). The outlier data are not shown in (b)–(d). Theoretical double-spike contamination curve (vertical line) was calculated based on the isotopic composition of NIST SRM 915a and ^{43}Ca-^{48}Ca double-spike listed in Table 1. Selective depletion of ^{40}Ca (the horizontal line in (a)) was modelled by decreasing $(^{40}Ca/^{44}Ca)_N$ arbitrarily. Range bars represent two standard error of the mean. [Colour figure can be viewed at wileyonlinelibrary.com]

fact that ^{48}Ca is the second brightest beam during the spiked runs and collected by the edge H4 Faraday cup. The ^{48}Ca ion beam with a large incident angle may hit the sides of the H4 collector and smooth its surface over time, which may cause the change in collector efficiency (Holmden and Bélanger 2010).

Mass-independent isotopic compositions of NIST SRM 915a

It is important to check whether internally corrected Ca isotopic ratios of NIST SRM 915a from different laboratories are consistent. Two hundred and thirty-seven runs of unspiked NIST SRM 915a yielded mean $(^{40}Ca/^{44}Ca)_N$ and $(^{43}Ca/^{44}Ca)_N$ values of 47.1516 ± 0.0096 (± 2.0 ε, 2*s*) and 0.064868 ± 0.000017 (± 2.6 ε, 2*s*), respectively (Table 1 and Figure 5b, c). Despite the time-dependent drift mentioned above, a long-term mean $(^{48}Ca/^{44}Ca)_N$ value for NIST SRM 915a was 0.0886516 ± 0.0000029 (2SE). This value is used for double-spike calibration and interlaboratory comparison. Our mean NIST SRM 915a $(^{40}Ca/^{44}Ca)_N$ is consistent with those (47.1519–47.1531) reported by Russell *et al.* (1978) and Simon *et al.* (2009), but significantly different from those reported by Caro *et al.* (2010), Naumenko-Dèzes *et al.* (2015) (47.1622 to 47.1649) and Huang *et al.* (2012) (*ca.* 47.134) (Figure S2a). Due to the single filament assembly adopted and low sample load, significant heterogeneous evaporation effect has been found by Naumenko-Dèzes *et al.* (2015). After a secondary correction using Equation (7) (above), Naumenko-Dèzes *et al.* (2015) reported NIST SRM 915a $(^{40}Ca/^{44}Ca)_N$ consistent with our value (Figure S2). Caro *et al.* (2010) did not report either $(^{43}Ca/^{44}Ca)_N$ or $(^{48}Ca/^{44}Ca)_N$ data, and a secondary correction is not allowed. Changing in β_{MC} during individual runs suggests that the higher $(^{40}Ca/^{44}Ca)_N$ reported by Caro *et al.* (2010) may be also due to uncorrected heterogeneous effect. No matter whether a secondary correction is applied,

$(^{40}Ca/^{44}Ca)_N$ values reported by Huang *et al.* (2012) are different from other studies (Russell *et al.* 1978, Simon *et al.* 2009, Naumenko-Dèzes *et al.* 2015, and this study). The reason remains unknown and is possibly due to the difference in mass spectrometers. An Isoprobe-T TIMS and a triple-filament assembly were used in Huang *et al.* (2012), while most other studies used a Triton-family TIMS. This interlaboratory difference may also originate from uncorrected cup efficiency difference. Combined with the well-known Faraday cup efficiency drift on Triton-family TIMS (Holmden and Bélanger 2010, Feng *et al.* 2015, Lehn and Jacobson 2015, this study), we suggest, at this stage, both mass-independent and mass-dependent Ca isotopic ratios should be reported relative to a common reference measurement standard measured simultaneously with unknown samples (e.g., NIST SRM 915a; Huang *et al.* 2012) rather than a certain specified value (e.g., $(^{40}Ca/^{44}Ca)_N$ of bulk silicate Earth (BSE) at 47.1487; Simon *et al.* 2009).

Intermediate measurement precision and measurement bias

Mass-independent Ca isotopic variations of twelve geological reference materials and NIST SRM 915a, including carbonate, seawater and rock reference materials ranging from peridotite to rhyolite, were measured and reported relative to the mean NIST SRM 915a value of each session as conventional ε values (Table 2). The intermediate precision of $\varepsilon^{40/44}Ca$, $\varepsilon^{43/44}Ca$ and $\varepsilon^{48/44}Ca$ for single mass-independent Ca isotopic measurement was ± 1.5, ± 3.0 and ± 2.8, respectively. Where each sample was measured more than eleven times, 2SE values for $\varepsilon^{40/44}Ca$, $\varepsilon^{43/44}Ca$ and $\varepsilon^{48/44}Ca$ were better than 0.30, 0.57 and 0.76, respectively. $\varepsilon^{40/44}Ca$ and $\varepsilon^{43/44}Ca$ for NIST SRM 915b from this study were -0.58 ± 0.08 (2SE) and 0.36 ± 0.16 (2SE), respectively, consistent with values (-1.2 ± 1.4 and -0.25 ± 0.91) recently reported by Naumenko-Dèzes *et al.* (2015) after a secondary correction to $^{48}Ca/^{44}Ca = 0.0886516$.

Mass-independent Ca isotopic compositions of geological reference materials

Twelve geological reference materials, including NIST SRM 915b, Atlantic seawater, one peridotite, three basalts, four intermediate to felsic igneous rocks, one carbonatite, and one sandstone yielded identical $\varepsilon^{43/44}Ca$ and $\varepsilon^{48/44}Ca$ values within ± 0.6. This provides a fundamental basis that terrestrial samples are fractionated from a single Ca isotopic composition (Appendix S1). Accordingly, different $\varepsilon^{40/44}Ca$ observed in these reference materials should reflect variable radiogenic ^{40}Ca enrichment.

Eleven of twelve geological reference materials showed $\varepsilon^{40/44}Ca$ within ± 1.1 relative to NIST SRM 915a. The granodiorite reference material GSP-2 with K/Ca ~ 3.05 (atomic ratio) showed a measurable ^{40}Ca enrichment with $\varepsilon^{40/44}Ca$ up to 4.04 ± 0.15 (2SE). Despite a high K/Ca ratio (up to 3.85), granite reference material GBW07103 (GSR-1) yielded a $\varepsilon^{40/44}Ca$ value of -0.35 ± 0.28 (2SE) and no detectable radiogenic ^{40}Ca ingrowth compared with peridotite and basalt reference materials. The emplacement age of GBW07103 and GSP-2 are unknown, but the former must be substantially younger than that of the latter. Previous studies have shown that only ancient samples with high K/Ca ratios may have significant ^{40}Ca enrichment, since ^{40}K has a very low relative abundance (*ca.* 0.12‰), while ^{40}Ca is the most abundant Ca isotope (Marshall and DePaolo 1989, Simon *et al.* 2009, Caro *et al.* 2010). Whether the commonly used reference material NIST SRM 915a has measurable radiogenic ^{40}Ca excess is still under debate (Simon *et al.* 2009, Caro *et al.* 2010, Fantle and Tipper 2014, Lehn and Jacobson 2015). For example, Simon *et al.* (2009) reported that BSE is slightly depleted in radiogenic ^{40}Ca with $\varepsilon^{40/44}Ca$ of -0.68 to -0.93, while Caro *et al.* (2010) measured eight ultramafic to mafic rocks that have $\varepsilon^{40/44}Ca$ around 0 relative to NIST SRM 915a within quoted errors. Peridotite JP-1 and other three basalts (BHVO-2, BCR-2 and GBW07105) yield $\varepsilon^{40/44}Ca$ ranging from -1.09 to -0.47, with an average of -0.79 ± 0.60 (2*s*), consistent with Simon *et al.* (2009). It is noted that these three studies rely on a totally different set of samples. However, at ± 1ε level, all studies found no measurable ^{40}Ca excess for NIST SRM 915a compared with most silicate rocks.

Stable isotopic compositions of geological materials

Optimisation of double-spike to sample Ca proportion

Measurement repeatability can be improved by optimising the spike-to-sample ratio in the spike-sample mixture (*q*) (Rudge *et al.* 2009, Lehn *et al.* 2013, Feng *et al.* 2015). The measurement repeatability of single double-spiked runs in this study was modelled after Lehn *et al.* (2013), assuming a total ion beam of 20 V, 120 cycles of static data acquisition in a single Faraday cup line and an integration time of 16.776 s. The modelled results are shown in Figure 6, which suggest an optimised *q* ranging from 0.05 to 0.20. This leads to a theoretical measurement repeatability on $\delta^{44/42}Ca$ of ~ 0.025‰. *q* was practically adopted to be 0.15 in this study. Twenty-eight runs of double-spiked NIST SRM 915a with a total ion beam within 20 ± 1 V yielded a mean measurement repeatability of 0.030 ± 0.014‰ (2*s*)

Table 2.
Mass-independent isotopic compositions of reference materials relative to NIST SRM 915a

Material	$\varepsilon^{40/44}Ca$	2*s*	2SE	$\varepsilon^{43/44}Ca$	2*s*	2SE	$\varepsilon^{46/44}Ca$	2*s*	2SE	$\varepsilon^{48/44}Ca$	2*s*	2SE	*n*
NIST SRM 915b	-0.58	1.26	0.08	0.36	1.99	0.16	2.3	101	4.8	-0.34	2.16	0.21	36
NIST SRM 915b (literature) [a]	-1.22		1.35	-0.25		0.91							
Atlantic seawater	-0.49	0.91	0.11	0.36	2.3	0.20	2.6	138	6.0	-0.11	2.08	0.27	20
Seawater1 (literature) [b]	-0.02		0.15										
Seawater2 (literature) [b]	-0.06		0.16										
Seawater3 (literature) [c]	-0.41		0.50	-0.04		1.34							
JP-1, peridotite	-0.47	1.93	0.14	0.27	3.23	0.27	-6.3	119	8.5	-0.47	2.38	0.33	34
BHVO-2, basalt	-0.60	1.68	0.14	0.27	3.27	0.29	2.7	117	9.1	-0.48	2.85	0.37	35
BHVO-2 (literature) [d]	1.1		1.6										
BCR-2, basalt	-1.09	1.75	0.15	-0.18	3.06	0.31	-4.7	122	9.9	-0.48	2.36	0.38	28
BCR-1 (literature) [c]	0.1		0.6	0.3		1.2				0.7		0.9	
BCR-1 (literature) [e]	-0.56		0.26	0.37		0.39							
GBW07105, basalt	-0.98	2.02	0.30	-0.27	4.55	0.57	3.7	222	20	-0.46	4.42	0.76	11
AGV-2, andesite	-0.82	1.91	0.24	-0.54	1.58	0.44	-20	131	13	0.09	2.55	0.58	12
GBW07104, andesite	-0.24	1.31	0.24	-0.43	5.17	0.47	-8.9	213	15	0.01	4.16	0.62	13
GSP-2, granodiorite	4.04	1.24	0.15	0.07	3.02	0.30	-16	120	9	-0.36	2.73	0.37	25
GBW07103, granite	-0.35	1.20	0.28	-0.57	3.81	0.55	-0.9	196	18	-0.08	4.52	0.66	12
COQ-1, carbonatite	0.15	1.90	0.16	0.07	2.37	0.32	-4.9	118	9.6	0.08	2.68	0.38	24
GBW07106, Quartz sandstone	0.49	1.14	0.26	-0.04	2.86	0.5	13	160	17	-0.28	3.88	0.60	11

Raw data are listed in Table S2, and ε values are calculated relative to the mean values of NIST SRM 915a for each session. Literature data sources: a, Naumenko-Dèzes *et al.* (2015); b, Caro *et al.* (2010); c, Huang *et al.* (2012); d, Amini *et al.* (2009); e, Simon *et al.* (2009).

for $\delta^{44/42}$Ca, comparable to the theoretical prediction. One over-spiked run with q = 0.275 and another under-spiked run with q = 0.039 yielded $\delta^{44/42}$Ca values of 0.00 ± 0.02‰ and 0.00 ± 0.03‰, respectively. This confirms the wide range of optimised q for high precision and accuracy predicted by the theoretical calculations (Figure 6).

Intermediate measurement precision and measurement bias

Intermediate measurement precision and accuracy for stable Ca isotopic determinations were estimated based on duplicate results of geological reference materials and interlaboratory comparison. Most previous studies use $\delta^{44/40}$Ca to report mass-dependent Ca isotopic variation. Because of possible radiogenic ^{40}Ca contribution (see Mass-independent isotopic compositions of geological materials), we used $\delta^{44/42}$Ca. Published $\delta^{44/40}$Ca data were re-calculated to $\delta^{44/42}$Ca using the equation $\delta^{44/42}Ca = (\delta^{44/40}Ca + \varepsilon^{40/44}Ca/10)/2.0483$, and mass-independent isotopic compositions are reported in Table 2. Mean $\delta^{44/42}$Ca values for NIST SRM 915a, 915b and Atlantic seawater from each measurement session during the period May 2015 to December 2015 are listed in Table S3 and plotted in Figure 7. No long-term drift was observed for $\delta^{44/42}$Ca at the ± 0.09 level. Based on 286 double-spiked runs of NIST SRM 915a, the intermediate precision of $\delta^{44/42}$Ca was 0.09‰ for single measurement, slightly better than those reported for stable Ca measurement using a ^{43}Ca-^{48}Ca double-spike recently (0.09‰ to 0.17‰ for $\delta^{44/42}$Ca) (Huang *et al.* 2010, Lehn and Jacobson 2015). Intermediate precision ('external') can be improved by multiple analyses of the same sample (Poitrasson and Freydier 2005, He *et al.* 2015). Each dissolved rock powder reference material was therefore measured on average eight times, and the mean values with 2SE are reported. This led to an average $\delta^{44/42}$Ca intermediate precision of 0.03‰, based on the duplicate measurements on ten rock reference materials (Table 3). Comparison of results with literature data was performed on the same basis (Table 3 and Figure 8). For example, the mean $\delta^{44/42}$Ca value for Atlantic seawater was 0.907 ± 0.007‰ (2SE, n = 147), consistent with the median value, 0.904‰, compiled by Fantle and Tipper (2014).

$\delta^{44/40}$Ca was also obtained by our ^{43}Ca-^{48}Ca double-spike measurements, which allowed $\varepsilon^{44/40}$Ca to be calculated using the double-spiked runs (Farkaš *et al.* 2011). It is important to assess the measurement precision and bias of $\varepsilon^{40/44}$Ca obtained using this approach. Based on

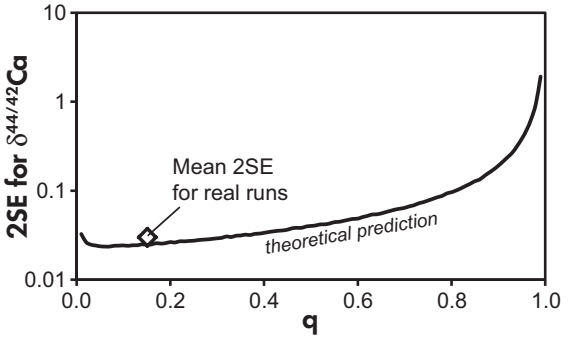

Figure 6. Theoretical $\delta^{44/42}$Ca measurement repeatability (2SE) using the ^{43}Ca-^{48}Ca double-spike from this study. The model reflects a 20-V total beam and 120 cycles with an integration time of 16.776 s. q, representative of the mole fraction of double-spike in the mixture, was adopted to be 0.15 in this study. Twenty-eight runs of double-spiked NIST SRM 915a with a total beam within 20 ± 1 V yielded a mean measurement repeatability of 0.030 ± 0.014‰ (2s), comparable to the theoretical prediction.

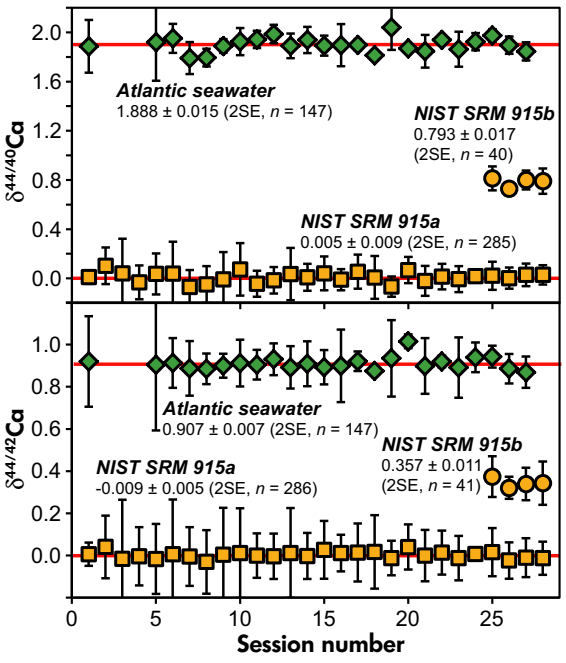

Figure 7. Intermediate measurement precision of stable Ca isotopic determinations exhibited by the mean values of NIST SRM 915a, 915b and Atlantic seawater from each session. Range bars represent two standard deviations. Horizontal lines are the true and recommended values for NIST SRM 915a and Atlantic seawater, respectively. Recommended values for Atlantic seawater are the median of the compilation from Fantle and Tipper (2014). [Colour figure can be viewed at wileyonlinelibrary.com]

Table 3.
Stable isotopic compositions of geological reference materials relative to NIST SRM 915a

Sample/ laboratory ID	$\delta^{44/40}$Ca	2*s*	2SE	$\delta^{44/42}$Ca	2*s*	2SE	$\varepsilon^{40/44}$Ca	2*s*	2SE	*n*	Data sources
Atlantic SW	1.888	0.183	0.015	0.907	0.082	0.007	-0.31	1.89	0.16	147	This study
Seawater (literature)	1.900		0.025	***0.904*** [a]		***0.013***					Compilation from Fantle and Tipper (2014)
SRM915b	0.793	0.105	0.017	0.357	0.069	0.011	-0.60	0.98	0.16	41	This study
SRM915b (literature)	0.72	0.11	0.02	***0.323*** [a]		***0.010***					TIMS, ^{42}Ca-^{48}Ca; Feng *et al.* (2016)
SRM915b (literature)	0.695	0.234	0.054	0.345	0.136	0.031				19	TIMS, ^{43}Ca-^{48}Ca; Lehn and Jacobson (2015)
SRM915b (literature)	0.731		0.006	***0.329*** [a]		***0.005***				37	TIMS, ^{42}Ca-^{43}Ca; Lehn *et al.* (2013)
SRM915b (literature)	0.72	0.22	0.04	***0.323*** [a]		***0.020***				56	TIMS, ^{43}Ca-^{48}Ca; Heuser and Eisenhauer (2008)
SRM915b (literature)				0.35		0.01				74	SSB, MC-ICP-MS; Valdes *et al.* (2014)
SRM915b (literature)				0.340	0.06	0.015				15	SSB, MC-ICP-MS; Harouaka *et al.* (2016)
SRM915b (literature)				0.42		0.02					SSB, MC-ICP-MS; Schiller *et al.* (2012)
SRM915b (RV)				***0.334***		***0.004***					
JP-1, peridotite											
He89	1.174	0.065	0.025	0.551	0.040	0.015	-0.46	1.12	0.42	7	This study
He139	1.093	0.079	0.026	0.536	0.123	0.041	0.05	2.25	0.75	9	This study
He101	1.219	0.128	0.043	0.524	0.118	0.039	-1.46	1.88	0.63	9	This study
He122	1.083	0.087	0.031	0.503	0.066	0.023	-0.54	1.67	0.59	8	This study
Weighted mean	**1.134**			**0.535**			**-0.61**				
2*s*	**0.131**			**0.041**			**1.26**				
2SE	0.015			0.012			0.28				
MSWD	**3.94**			**1.04**							
JP-1 (literature)	1.15	0.07	0.03	***0.538*** [a]		***0.016***				4	TIMS, ^{42}Ca-^{43}Ca; Magna *et al.* (2015)
JP-1 (RV)				***0.536***		***0.009***					
BHVO-2, basalt											
He52	0.759	0.044	0.015	0.384	0.055	0.018	0.27	0.95	0.32	9	This study
He115	0.777	0.133	0.054	0.349	0.074	0.030	-0.63	1.04	0.42	6	This study
He102	0.826	0.210	0.074	0.388	0.130	0.046	-0.32	1.52	0.54	8	This study
He108	0.723	0.116	0.039	0.348	0.105	0.035	-0.11	1.54	0.51	9	This study
He140	0.828	0.171	0.057	0.382	0.095	0.032	-0.46	1.43	0.48	9	This study
He141	0.821	0.056	0.019	0.378	0.095	0.032	-0.46	1.88	0.63	9	This study
He142	0.850	0.091	0.032	0.381	0.084	0.030	-0.70	1.54	0.54	8	This study
Weighted mean	**0.787**			**0.375**			**-0.24**				
2*s*	**0.091**			**0.034**			**0.67**				
2SE	0.010			0.011			0.17				
MSWD	**2.39**			**0.30**							
BHVO-1 (literature)	1.00		0.12	0.49		0.17					TIMS, ^{43}Ca-^{48}Ca; Huang *et al.* (2010)
BHVO-1 (literature)	0.96		0.05	0.44		0.03					TIMS, ^{43}Ca-^{48}Ca; Huang *et al.* (2011)
BHVO-1 (literature)				0.50		0.03					SSB, MC-ICP-MS; Schiller *et al.* (2012)
BHVO-1 (literature)	0.804	0.203	0.083	0.417	0.115	0.028				6	TIMS, ^{43}Ca-^{48}Ca; Lehn and Jacobson (2015)

Table 3 (continued).
Stable isotopic compositions of geological reference materials relative to NIST SRM 915a

Sample/ laboratory ID	$\delta^{44/40}$Ca	2*s*	2SE	$\delta^{44/42}$Ca	2*s*	2SE	$\varepsilon^{40/44}$Ca	2*s*	2SE	*n*	Data sources
BHVO-1 (literature)	0.780	0.033	0.014	***0.352*** [a]		***0.010***				6	TIMS, ^{42}Ca-^{43}Ca; Lehn and Jacobson (2015)
BHVO-1 (literature)	0.77	0.10	0.03	***0.347*** [a]		***0.029***				3	TIMS, ^{42}Ca-^{48}Ca; Feng *et al.* (2016)
BHVO-2 (literature)	0.77	0.10	0.03	***0.347*** [a]		***0.016***				12	TIMS, ^{42}Ca-^{48}Ca; Feng *et al.* (2016)
BHVO-2 (literature)	0.90	0.11	0.05	***0.41*** [a]		***0.03***				5	TIMS, ^{42}Ca-^{43}Ca; Magna *et al.* (2015)
BHVO-2 (literature)				0.41		0.01					SSB, MC-ICP-MS; Valdes *et al.* (2014)
BHVO-2 (literature)	0.75	0.22	0.05	***0.34*** [a]		***0.03***				20	TIMS, ^{42}Ca-^{43}Ca; Amini *et al.* (2009)
BHVO-2 (literature)	0.90			***0.41*** [a]							TIMS, ^{42}Ca-^{43}Ca; Amini *et al.* (2009)
BHVO-2 (literature)				0.46		0.04					SSB, MC-ICP-MS; Schiller *et al.* (2012)
BHVO-1(RV)				***0.364***		***0.008***					
BHVO-2(RV)				***0.381***		***0.007***					
BCR-2, basalt											
He90	0.839	0.145	0.048	0.423	0.078	0.026	0.27	1.47	0.49	9	This study
He116	0.816	0.173	0.087	0.380	0.068	0.034	-0.37	1.29	0.65	4	This study
He103	0.792	0.157	0.052	0.356	0.087	0.029	-0.64	2.15	0.72	9	This study
He109	0.785	0.077	0.027	0.371	0.066	0.023	-0.26	1.34	0.47	8	This study
Weighted mean	**0.798**			**0.383**			**-0.17**				
2*s*	**0.049**			**0.058**			**0.76**				
2SE	0.021			0.014			0.28				
MSWD	**0.33**			**1.17**							
BCR-1 (literature)	0.73		0.05	***0.30*** [a]		***0.03***					TIMS, ^{42}Ca-^{48}Ca; Simon and DePaolo (2010)
BCR-2 (literature)				0.41		0.09					SSB, MC-ICP-MS; Valdes *et al.* (2014)
BCR-2 (literature)	0.79	0.12	0.02	***0.332*** [a]		***0.014***				24	TIMS, ^{42}Ca-^{48}Ca; Feng *et al.* (2016)
BCR-2 (literature)	0.81	0.17	0.07	***0.34*** [a]		***0.03***				6	TIMS, ^{42}Ca-^{43}Ca; Amini *et al.* (2009)
BCR-2 (literature)	0.93			***0.40*** [a]							TIMS, ^{42}Ca-^{43}Ca; Amini *et al.* (2009)
BCR-2 (literature)	0.92	0.40	0.20	***0.40*** [a]		***0.10***				4	TIMS, ^{43}Ca-^{48}Ca; Wombacher *et al.* (2009)
BCR-2 (literature)				0.50		0.04					SSB, MC-ICP-MS; Schiller *et al.* (2012)
BCR-2(RV)				***0.359***		***0.009***					
GBW07105 (GSR-3), basalt											
He144	0.566	0.065	0.022	0.255	0.082	0.027	-0.43	1.61	0.54	9	This study
He226	0.633	0.088	0.031	0.269	0.047	0.017	-0.82	0.70	0.25	8	This study
Weighted mean	**0.587**			**0.265**			**-0.76**				
2*s*	**0.095**			**0.020**			**0.55**				
2SE	0.018			0.014			0.22				
MSWD	**3.14**			**0.19**							
AGV-2, andesite											
He54	0.785	0.06	0.02	0.371	0.07	0.02	-0.37	0.72	0.29	9	This study
He111	0.679	0.12	0.05	0.335	0.12	0.05	0.07	2.01	0.82	6	This study
He104	0.676	0.14	0.05	0.332	0.07	0.02	0.05	1.39	0.46	9	This study
Weighted mean	**0.751**			**0.349**			**-0.23**				

Table 3 (continued).
Stable isotopic compositions of geological reference materials relative to NIST SRM 915a

Sample/ laboratory ID	$\delta^{44/40}$Ca	2*s*	2SE	$\delta^{44/42}$Ca	2*s*	2SE	$\varepsilon^{40/44}$Ca	2*s*	2SE	*n*	Data sources
2*s*	**0.124**			**0.044**			**0.50**				
2SE	0.019			0.015			0.24				
MSWD	**3.57**			**0.76**							
AGV-2 (literature)				0.37		0.05					SSB, MC-ICP-MS; Valdes *et al.* (2014)
AGV-2 (literature)	0.79	0.09	0.03	***0.346*** [a]		***0.019***				9	TIMS, ^{42}Ca-^{48}Ca; Feng *et al.* (2016)
AGV-2(RV)				***0.349***		***0.012***					
GBW07104 (GSR-2), andesite											
He144	0.664	0.124	0.041	0.317	0.126	0.042	-0.15	2.06	0.69	9	This study
He225	0.691	0.118	0.042	0.305	0.053	0.019	-0.66	0.83	0.29	8	This study
Weighted mean	**0.677**			**0.307**			**-0.58**				
2*s*	**0.037**			**0.017**			**0.72**				
2SE	0.029			0.017			0.27				
MSWD	**0.20**			**0.07**							
GSP-2, granodiorite											
He105 GSP-2	0.294	0.169	0.056	0.308	0.082	0.027	3.37	1.44	0.48	9	This study
He229 GSP-2	0.299	0.036	0.013	0.322	0.047	0.017	3.62	1.05	0.37	8	This study
He230 GSP-2	0.270	0.091	0.032	0.315	0.047	0.017	3.75	0.52	0.19	8	This study
Weighted mean	**0.295**			**0.317**			**3.69**				
2*s*	**0.031**			**0.014**			**0.39**				
2SE	0.012			0.011			0.16				
MSWD	**0.35**			**0.12**							
GBW07103 (GSR-1), granite											
He143	0.727	0.135	0.045	0.384	0.085	0.028	0.59	1.40	0.47	9	This study
He224	0.750	0.045	0.016	0.364	0.028	0.010	-0.05	0.65	0.23	8	This study
Weighted mean	**0.747**			**0.366**			**0.07**				
2*s*	**0.032**			**0.029**			**0.91**				
2SE	0.015			0.009			0.21				
MSWD	**0.23**			**0.45**							
COQ-1, carbonatite											
He90	0.672	0.039	0.022	0.304	0.098	0.057	-0.49	1.76	1.02	3	This study
He113	0.731	0.093	0.042	0.337	0.073	0.030	-0.28	0.92	0.41	6	This study
He119 [b]	0.614		0.16	0.350		0.09	1.04			1	This study
He106	0.746	0.141	0.050	0.335	0.092	0.033	-0.60	2.13	0.75	8	This study
Weighted mean	**0.659**			**0.335**			**-0.37**				
2*s*	**0.121**			**0.039**			**0.33**				
2SE	0.014			0.019			0.34				
MSWD	**3.68**			**0.14**							

Table 3 (continued).
Stable isotopic compositions of geological reference materials relative to NIST SRM 915a

Sample/ laboratory ID	$\delta^{44/40}Ca$	2*s*	2SE	$\delta^{44/42}Ca$	2*s*	2SE	$\varepsilon^{40/44}Ca$	2*s*	2SE	*n*	Data sources
COQ-1 (literature)	0.71	0.11	0.06	***0.354*** [a]		***0.028***				4	TIMS, ^{42}Ca-^{48}Ca; Feng *et al.* (2016)
COQ-1(RV)				***0.341***		***0.015***					
GBW07106, sandstone											
He146	0.379	0.092	0.031	0.216	0.111	0.037	0.64	1.90	0.63	9	This study
He228	0.439	0.124	0.047	0.221	0.056	0.021	0.13	0.85	0.32	7	This study
Weighted mean	**0.397**			**0.220**			**0.24**				
2*s*	**0.085**			**0.007**			**0.71**				
2SE	0.026			0.018			0.29				
MSWD	**0.38**			**0.00**							

Superscript a denotes $\delta^{44/42}Ca$ values calculated by ($\delta^{44/40}Ca + \varepsilon^{40/44}Ca/10$)/2.0483 with correction for the radiogenic ^{40}Ca anomaly obtained here, where only $\delta^{44/40}Ca$ has been previously reported. Literature data for seawater represent median values of the data compilation from Fantle and Tipper (2014). He119 (COQ-1) was only measured on TIMS one time, and intermediate precision for single measurement is given for the errors. These data were not used to calculate the mean value and standard deviation for $\varepsilon^{40/44}Ca$. Recommended values (RV) are given, if consistent data from at least two independent laboratories were integrated.

duplicated measurements of double-spiked NIST SRM 915a, 915b and Atlantic seawater, the intermediate precision of $\varepsilon^{40/44}Ca$ was between 1.0 and 1.9 for single measurements (Table S3), comparable to that of unspiked runs (see Time-dependent drift of Faraday cup efficiency). Duplicate analyses of ten rock reference material powders indicate that intermediate precision for $\varepsilon^{40/44}Ca$ could be better than 1.0, with an average of 0.68, provided each sample was analysed eight times (Table 3). $\varepsilon^{40/44}Ca$ values calculated using the double-spiked runs were consistent within ± 1.0 with those measured in independent unspiked runs (Figure 9). In summary, $\delta^{44/42}Ca$ and $\varepsilon^{44/40}Ca$ could be measured simultaneously within ± 0.03‰ and ± 1.0, respectively, if each sample was analysed eight times using a ^{43}Ca-^{48}Ca double-spike technique and the data processing procedures reported here.

Stable Ca isotopic compositions of geological reference materials

We report stable Ca isotopic compositions of twelve commonly used geological reference materials relative to NIST SRM 915a (Table 3). As noted above, these data are in general consistent with the literature data within quoted errors after correction of radiogenic ^{40}Ca contribution. Combined with literature data, new values have been calculated for eleven of twelve reference materials as error-weighted means after Craddock and Dauphas (2010) and listed in Table 3. Data from Schiller *et al.* (2012) were not integrated, because they are systematically higher than other published values. No further update for recommended values of the seawater is necessary since the data reported here are very close to the median of the literature data (Table 3; Fantle and Tipper 2014).

Nine igneous rocks yielded $\delta^{44/42}Ca$ values ranging from 0.265 ± 0.014‰ (2SE) to 0.536 ± 0.009‰ (2SE), demonstrating a detectable stable Ca isotope fractionation during high-temperature processes. Carbonatite COQ-1 has a $\delta^{44/42}Ca$ of 0.335 ± 0.019‰ (2SE), similar to the value (~ 0.35‰) previously reported by Feng *et al.* (2016). Three basaltic reference materials, BHVO-2, BCR-2 and GBW07105, have $\delta^{44/42}Ca$ from 0.265 ± 0.014‰ (2SE) to 0.381 ± 0.007‰ (2SE), systematically lower than peridotite JP-1 (0.536 ± 0.009‰; 2SE). This is consistent with the previous observation that basalts have stable Ca isotopic compositions lighter than the mean upper mantle (Figure 10) (Huang *et al.* 2010, 2011, Valdes *et al.* 2014). Significant lower and variable $\delta^{44/42}Ca$ observed in Hawaii basalts have been attributed to incorporating surface carbonates enriched in isotopically light Ca into their mantle sources (Huang *et al.* 2011). Recycled carbonates can be

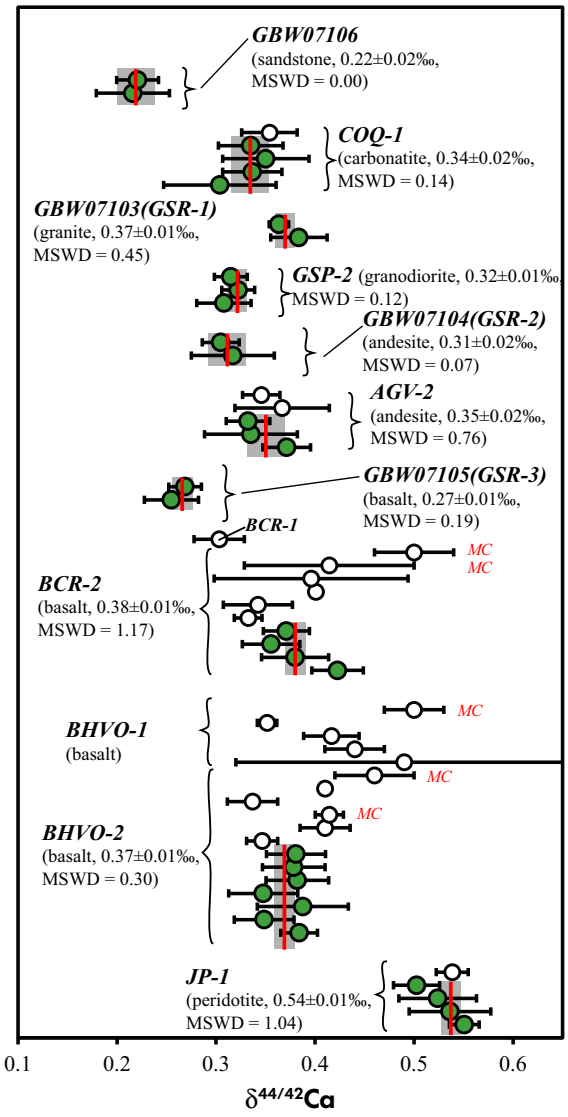

Figure 8. Summary of stable Ca isotopic compositions of geological reference materials. Ca isotopic data obtained in this study (filled symbols) are compared against literature data (open symbols). The weighted mean values and their relevant errors of our own data are plotted as (vertical) red lines and grey bars. All the literature data were converted to the $\delta^{44/42}$Ca scale using $\delta^{44/42}Ca = (\delta^{44/42}Ca + \varepsilon^{40/44}Ca/10)/2.0483$ if only $\delta^{44/40}$Ca has been reported. 'MC' indicates data obtained by MC-ICP-MS. Data sources refer to Table 3, and range bars represent two standard error of the mean. [Colour figure can be viewed at wileyonlinelibrary.com]

identified by the elevated Sr/Nb in basalts (Huang *et al.* 2011). GBW07105, a Cenozoic basalt from Zhangjiakou, eastern China, with the lowest $\delta^{44/42}$Ca, however, does not have high Sr/Nb (Figure 10c), indicating that low $\delta^{44/42}$Ca magmas may be produced by other processes.

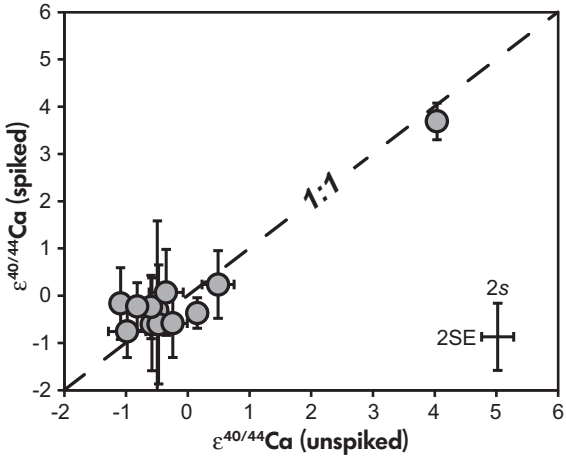

Figure 9. A comparison of $\varepsilon^{40/44}$Ca obtained for geological reference materials from the results of ^{43}Ca-^{48}Ca double-spiked and unspiked runs.

It is still under debate whether Ca isotopes fractionate during magma differentiation due to limited high-precision Ca isotopic data of differentiated magmas with known elemental compositions. Data for intermediate to felsic geological reference materials measured in this and previous studies (Amini *et al.* 2009, Valdes *et al.* 2014, Feng *et al.* 2016) allow a first-order constraint on this issue. Four intermediate to felsic igneous reference materials (AGV-2, GSP-2, GBW07103 and GBW07104) have highly variable CaO from 5.20% *m/m* to 1.55% *m/m*, but only reveal a limited $\delta^{44/42}$Ca variation from 0.307 ± 0.017‰ (2SE) to 0.366 ± 0.009‰ (2SE). Combined with literature data, similar to the compilation of Schiller *et al.* (2016), no trend can be identified between $\delta^{44/42}$Ca and MgO, CaO for mafic to felsic geological reference materials (Figure 10a, b), suggesting that Ca isotope fractionation is either insignificant or not systematic (e.g., crystallisation of different minerals has opposite isotopic effect) during magma differentiation. Plagioclase is a major Ca-rich mineral in additional to pyroxene and amphibole. Substantial plagioclase crystallisation decreases the Eu*, defined as $Eu/\sqrt{(Sm \times Gd)}$ normalised to CI chondrite values of magmas. The lack of correlation between $\delta^{44/42}$Ca and Eu* (Figure 10d) may further suggest insignificant Ca isotope fractionation during fractional crystallisation of plagioclase. All mafic to felsic igneous samples with light Ca isotopic compositions tend to have high (Dy_n/Yb_n) (Figure 10e), an indicator of residual garnet (He *et al.* 2011) or garnet crystallisation during differentiation (Macpherson *et al.* 2006). Garnet has a stronger Ca-O bond than clinopyroxene and thus likely has substantially heavier Ca isotopes than clinopyroxene and other Ca-rich minerals (e.g., amphibole and plagioclase) (Magna *et al.*

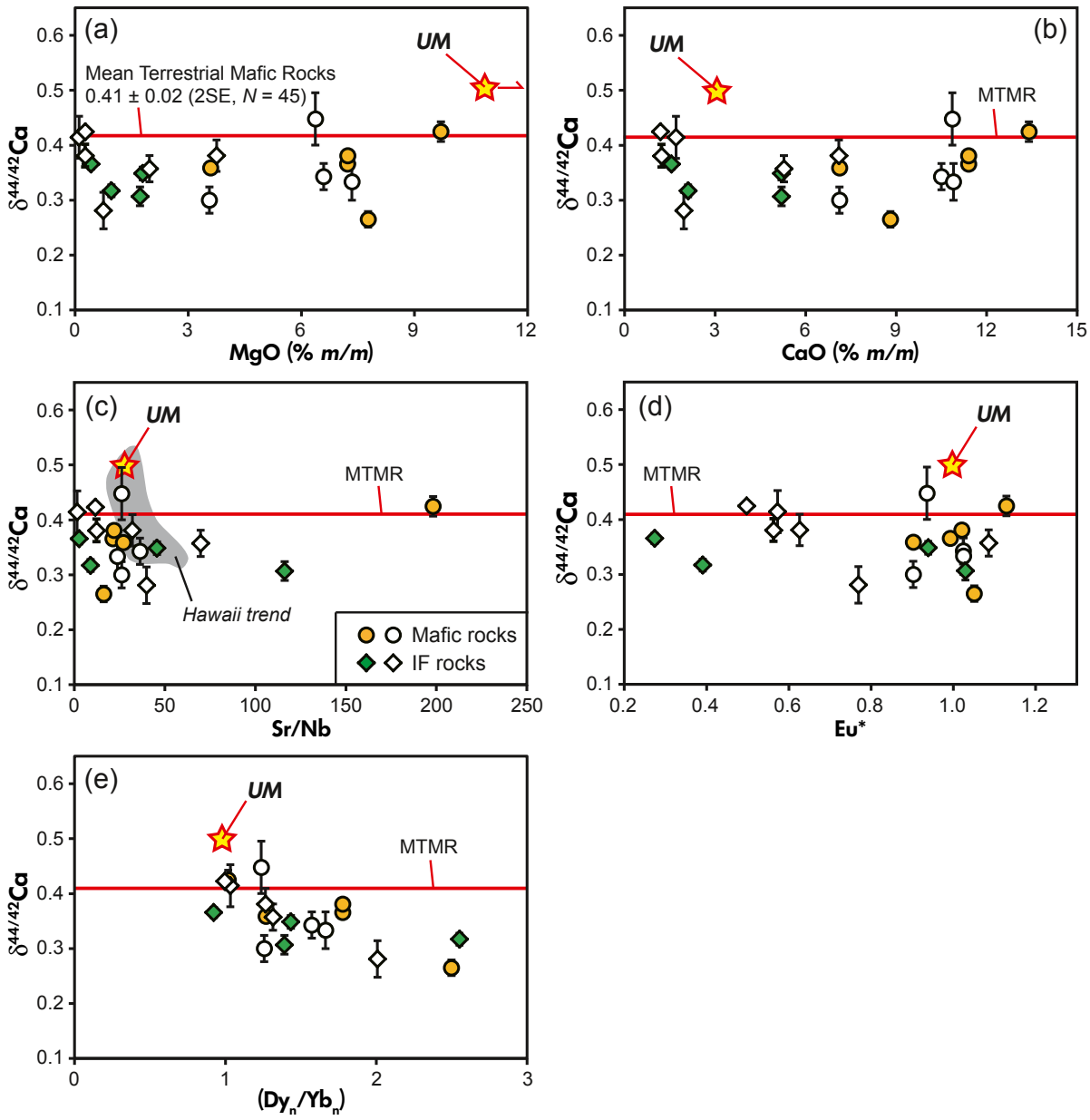

Figure 10. $\delta^{44/42}$Ca vs. MgO, CaO, Sr/Nb, Eu* and (Dy_n/Yb_n) diagrams for mafic and intermediate to felsic (IF) igneous reference materials. Newly reported data and those compiled from at least two independent laboratories (filled) as well as the literature data from only one laboratory (open) are plotted. Mean terrestrial basaltic rock was calculated from forty-five mafic rocks recently reported (Amini *et al.* 2009, Huang *et al.* 2010, 2011, Simon and DePaolo 2010, Valdes *et al.* 2014, Jacobson *et al.* 2015). The upper mantle estimate is from Huang *et al.* (2010) and Sun and McDonough (1989). Eu* = $Eu_N/\sqrt{(Sm_N*Gd_N)}$ where subscript *N* represents normalisation to the chondrite values (Sun and McDonough 1989). The Hawaii trend is after Huang *et al.* (2011). Elemental data for geological reference materials are from the GeoReM database (http://georem.mpch-mainz.gwdg.de) and the certificates from IGGE and USGS. [Colour figure can be viewed at wileyonlinelibrary.com]

2015). Partial melting with abundant residual garnet and/or magma differentiation with substantial crystalline garnet may be another way to produce low $\delta^{44/42}$Ca magmas.

The commonly used certified reference material NIST SRM 915a has been exhausted and replaced by NIST SRM 915b. Therefore, it is important to calibrate NIST SRM 915b

relative to NIST SRM 915a. Six of seven laboratories yielded consistent $\delta^{44/42}$Ca values for NIST SRM 915b ranging from 0.323 ± 0.010‰ (2SE) to 0.357 ± 0.011‰ (2SE), with a new recommended value of 0.334 ± 0.004‰ (2SE). Again, the data from Schiller *et al.* (2012) are significantly higher than others and were not included. Compared with NIST SRM 915a, NIST SRM 915b has both mass-independent and mass-dependent Ca isotopic compositions closer to the BSE estimates represented by peridotites and basalts (Tables 2 and 3). The only sedimentary reference material in our study, sandstone GBW07106, has a $\delta^{44/42}$Ca of 0.220 ± 0.018‰ (2SE), lower than those of all igneous reference materials reported.

Concluding remarks

This study presents a ^{43}Ca-^{48}Ca double-spike calibration procedure, TIMS measurement procedures for Ca isotopic composition and reports Ca isotopic compositions for thirteen geological reference materials. Using our double-spike technique, $\delta^{44/42}$Ca and $\varepsilon^{40/44}$Ca could be measured simultaneously with a precision of ± 0.03‰ and ± 1.0, respectively, provided that each sample was analysed eight times. We provide a comprehensive data set of both mass-independent and mass-dependent Ca isotopic compositions of thirteen geological reference materials. This will allow future interlaboratory calibration of Ca isotopic measurement.

Measurement of igneous reference materials yielded $\delta^{44/42}$Ca values between 0.27‰ and 0.54‰ relative to NIST SRM 915a, well outside the intermediate precision of the measurements. Basaltic to felsic rocks generally have 'lighter' Ca isotopic compositions than the upper mantle to different extents. Therefore, either significant Ca isotope fractionation occurs during magmatic processes, or the variation can be attributed to recycling of surface materials. No correlation between $\delta^{44/42}$Ca and MgO or CaO was observed for mafic to felsic igneous reference materials, suggesting that Ca isotope fractionation is either insignificant or not systematic during magma differentiation. Given the rather low $\delta^{44/42}$Ca for a sandstone and that the lower $\delta^{44/42}$Ca reference materials tend to have higher (Dy_n/Yb_n), we suggest a potential role for residual or crystalline garnet and incorporation of silicate sediments into sources to produce magmas with low $\delta^{44/42}$Ca.

Acknowledgements

Constructive comments from two anonymous reviewers and efficient editorial handling of Mary Horan are highly appreciated. This work was supported by the National Natural Science Foundation of China (41230209 to LSG, 41473016 and 41673012 to YSH) and the State Key Laboratory of Geological Processes and Mineral Resources (Open Research Program GPMR201510). SCH acknowledges support from NSF Award EAR-1524387. This is CUGB petrogeochemical contribution No. PGC-201514.

References

Amini M., Eisenhauer A., Bohm F., Holmden C., Kreissig K., Hauff F. and Jochum K.P. (2009)
Calcium isotopes ($\delta^{44/40}$Ca) in MPI-DING reference glasses, USGS rock powders and various rocks: Evidence for Ca isotope fractionation in terrestrial silicates. **Geostandards and Geoanalytical Research, 33**, 231–247.

Boulyga S.F. (2010)
Calcium isotope analysis by mass spectrometry. **Mass Spectrometry Reviews, 29**, 685–716.

Caro G., Bourdon B., Birck J.-L. and Moorbath S. (2003)
^{146}Sm-^{142}Nd evidence from Isua metamorphosed sediments for early differentiation of the Earth's mantle. **Nature, 423**, 428–432.

Caro G., Papanastassiou D.A. and Wasserburg G.J. (2010)
^{40}K–^{40}Ca isotopic constraints on the oceanic calcium cycle. **Earth and Planetary Science Letters, 296**, 124–132.

Craddock P.R. and Dauphas N. (2010)
Iron isotopic compositions of geological reference materials and chondrites. **Geostandards and Geoanalytical Research, 35**, 101–123.

De La Rocha C.L. and DePaolo D.J. (2000)
Isotopic evidence for variations in the marine calcium cycle over the Cenozoic. **Science, 289**, 1176–1178.

Fantle M.S. and Bullen T.D. (2009)
Essentials of iron, chromium, and calcium isotope analysis of natural materials by thermal ionization mass spectrometry. **Chemical Geology, 258**, 50–64.

Fantle M.S. and Tipper E.T. (2014)
Calcium isotopes in the global biogeochemical Ca cycle: Implications for development of a Ca isotope proxy. **Earth-Science Reviews, 129**, 148–177.

Farkaš J., Böhm F., Wallmann K., Blenkinsop J., Eisenhauer A., van Geldern R., Munnecke A., Voigt S. and Veizer J. (2007)
Calcium isotope record of Phanerozoic oceans: Implications for chemical evolution of seawater and its causative mechanisms. **Geochimica et Cosmochimica Acta, 71**, 5117–5134.

Farkaš J., Déjeant A., Novák M. and Jacobsen S.B. (2011)
Calcium isotope constraints on the uptake and sources of Ca^{2+} in a base-poor forest: A new concept of combining stable ($\delta^{44/42}$Ca) and radiogenic (εCa) signals. **Geochimica et Cosmochimica Acta, 75**, 7031–7046.

references

Feng L.P., Zhou L., Yang L., Tong S.Y., Hu Z.C. and Gao S. (2015)
Optimization of the double spike technique using peak jump collection by a Monte Carlo method: An example for the determination of Ca isotope ratios. Journal of Analytical Atomic Spectrometry, 30, 2403–2411.

Feng L.P., Zhou L., Yang L., DePaolo D.J., Tong S.Y., Liu Y.S., Owens T.L. and Gao S. (2016)
Calcium isotopic compositions of sixteen USGS reference materials. Geostandards and Geoanalytical Research. doi:10.1111/ggr.12131.

Fletcher I.R., Maggi A.L., Rosman K.J.R. and McNaughton N. (1997)
Isotopic abundance measurements of K and Ca using a wide-dispersion multi-collector mass spectrometer and low-fractionation ionisation techniques. International Journal of Mass Spectrometry and Ion Processes, 163, 1–17.

Harouaka K., Mansor M., Macalady J.L. and Fantle M.S. (2016)
Calcium isotopic fractionation in microbially mediated gypsum precipitates. Geochimica et Cosmochimica Acta, 184, 114–131.

Hart S.R. and Zindler A. (1989)
Isotope fractionation laws: A test using calcium. International Journal of Mass Spectrometry and Ion Processes, 89, 287–301.

He Y.S., Li S.G., Hoefs J., Huang F., Liu S.A. and Hou Z.H. (2011)
Post-collisional granitoids from the Dabie orogen: New evidence for partial melting of a thickened continental crust. Geochimica et Cosmochimica Acta, 75, 3815–3838.

He Y.S., Ke S., Teng F.Z., Wang T.T., Wu H.J., Lu Y.H. and Li S.G. (2015)
High-precision iron isotope analysis of geological reference materials by high-resolution MC-ICP-MS. Geostandards and Geoanalytical Research, 39, 341–356.

Heuser A. and Eisenhauer A. (2008)
The calcium isotope composition ($\delta^{44/40}$Ca) of NIST SRM 915b and NIST SRM 1486. Geostandards and Geoanalytical Research, 32, 311–315.

Heuser A., Eisenhauer A., Gussone N., Bock B., Hansen B.T. and Nägler T.F. (2002)
Measurement of calcium isotopes (δ^{44}Ca) using a multi-collector TIMS technique. International Journal of Mass Spectrometry, 220, 385–397.

Holmden C. and Bélanger N. (2010)
Ca isotope cycling in a forested ecosystem. Geochimica et Cosmochimica Acta, 74, 995–1015.

Huang S.C., Farkaš J. and Jacobsen S.B. (2010)
Calcium isotopic fractionation between clinopyroxene and orthopyroxene from mantle peridotites. Earth and Planetary Science Letters, 292, 337–344.

Huang S.C., Farkas J. and Jacobsen S.B. (2011)
Stable calcium isotopic compositions of Hawaiian shield lavas: Evidence for recycling of ancient marine carbonates into the mantle. Geochimica et Cosmochimica Acta, 75, 4987–4997.

Huang S.C., Farkaš J., Yu G., Petaev M.I. and Jacobsen S.B. (2012)
Calcium isotopic ratios and rare earth element abundances in refractory inclusions from the Allende CV3 chondrite. Geochimica et Cosmochimica Acta, 77, 252–265.

Jacobson A.D., Grace A.M., Lehn G.O. and Holmden C. (2015)
Silicate versus carbonate weathering in Iceland: New insights from Ca isotopes. Earth and Planetary Science Letters, 416, 132–142.

Johnson C.M. and Beard B.L. (1999)
Correction of instrumentally produced mass fractionation during isotopic analysis of Fe by thermal ionization mass spectrometry. International Journal of Mass Spectrometry, 193, 87–99.

Lehn G.O. and Jacobson A.D. (2015)
Optimization of a ^{48}Ca-^{43}Ca double-spike MC-TIMS method for measuring Ca isotope ratios ($\delta^{44/40}$Ca and $\delta^{44/42}$Ca): Limitations from filament reservoir mixing. Journal of Analytical Atomic Spectrometry, 30, 1571–1581.

Lehn G.O., Jacobson A.D. and Holmden C. (2013)
Precise analysis of Ca isotope ratios ($\delta^{44/40}$Ca) using an optimized ^{43}Ca–^{42}Ca double-spike MC-TIMS method. International Journal of Mass Spectrometry, 351, 69–75.

Li J., Zhu X.K. and Tang S.H. (2011)
The application of double spike in non-traditional stable isotopes: A case study on Mo isotopes. Rock and Mineral Analysis, 30, 138–143.

Macpherson C.G., Dreher S.T. and Thirlwall M.F. (2006)
Adakites without slab melting: High pressure differentiation of island arc magma, Mindanao, the Philippines. Earth and Planetary Science Letters, 243, 581–593.

Magna T., Gussone N. and Mezger K. (2015)
The calcium isotope systematics of Mars. Earth and Planetary Science Letters, 430, 86–94.

Marshall B.D. and DePaolo D.J. (1982)
Precise age determinations and petrogenetic studies using the K-Ca method. Geochimica et Cosmochimica Acta, 46, 2537–2545.

Marshall B.D. and DePaolo D.J. (1989)
Calcium isotopes in igneous rocks and the origin of granite. Geochimica et Cosmochimica Acta, 53, 917–922.

references

Morgan J.L.L., Gordon G.W., Arrua R.C., Skulan J.L., Anbar A.D. and Bullen T.D. (2011)
High-precision measurement of variations in calcium isotope ratios in urine by multiple collector inductively coupled plasma-mass spectrometry. Analytical Chemistry, 83, 6956–6962.

Naumenko-Dèzes M.O., Bouman C., Nägler T.F., Mezger K. and Villa I.M. (2015)
TIMS measurements of full range of natural Ca isotopes with internally consistent fractionation correction. International Journal of Mass Spectrometry, 387, 60–68.

Niederer F.R. and Papanastassiou D.A. (1984)
Ca isotopes in refractory inclusions. Geochemica et Cosmochimica Acta, 48, 1279–1293.

Poitrasson F. and Freydier R. (2005)
Heavy iron isotope composition of granites determined by high resolution MC-ICP-MS. Chemical Geology, 222, 132–147.

Rudge J.F., Reynolds B.C. and Bourdon B. (2009)
The double spike toolbox. Chemical Geology, 265, 420–431.

Russell W.A., Papanastassiou D.A. and Tombrello T.A. (1978)
Ca isotope fractionation on the Earth and other solar system materials. Geochimica et Cosmochimica Acta, 42, 1075–1090.

Schiller M., Paton C. and Bizzarro M. (2012)
Calcium isotope measurement by combined HR-MC-ICP-MS and TIMS. Journal of Analytical Atomic Spectrometry, 27, 38–49.

Schiller M., Gussone N. and Wombacher F. (2016)
High temperature Ca isotope geochemistry of terrestrial silicate rocks, minerals and melts. In: Gussone N., Schmitt A.D., Heuser A., Wombacher F., Dietzel M., Tipper E. and Schiller M. (eds), Calcium stable geochemistry. Springer (Berlin), 223–229.

Simon J.I. and DePaolo D.J. (2010)
Stable calcium isotopic composition of meteorites and rocky planets. Earth and Planetary Science Letters, 289, 457–466.

Simon J.I., DePaolo D.J. and Moynier F. (2009)
Calcium isotope composition of meteorites, Earth, and Mars. The Astrophysical Journal, 702, 707–715.

Sun S.S. and McDonough W.F. (1989)
Chemical and isotopic systematics of oceanic basalts: Implication for mantle composition and process. In: Saunders A.D. and Norry M.J. (eds), Magmatism in the ocean basins. Geological Society of London, Special Publication, 42, 313–345.

Tipper E., Galy A. and Bickle M. (2006)
Riverine evidence for a fractionated reservoir of Ca and Mg on the continents: Implications for the oceanic Ca cycle. Earth and Planetary Science Letters, 247, 267–279.

Valdes M.C., Moreira M., Foriel J. and Moynier F. (2014)
The nature of Earth's building blocks as revealed by calcium isotopes. Earth and Planetary Science Letters, 394, 135–145.

Wombacher F., Eisenhauer A., Heuser A. and Weyer S. (2009)
Separation of Mg, Ca and Fe from geological reference materials for stable isotope ratio analyses by MC-ICP-MS and double-spike TIMS. Journal of Analytical Atomic Spectrometry, 24, 627–636.

Zhu H.L., Zhang Z.F., Liu Y.F., Liu F. and Kang J.T. (2015)
Calcium isotope geochemistry review. Earth Science Frontiers, 22, 44–53.

Zhu H.L., Zhang Z.F., Liu Y.F., Fang L., Xin L. and Sun W.D. (2016)
Calcium isotopic fractionation during ion-exchange column chemistry and thermal ionisation mass spectrometry (TIMS) determination. Geostandards and Geoanalytical Research, 40, 185–194.

Supporting information

The following information may be found in the online version of this article:

Appendix S1. Data deduction procedures.

Figure S1. Measured $(^{40}Ca/^{44}Ca)_N$ from 100 theoretical cases with significant heterogeneous effect using a Monte Carlo approach.

Figure S2. Comparison of the absolute $^{40}Ca/^{44}Ca$ ratios observed in this study with the literature data.

Table S1. Raw data for unspiked NIST SRM 915a runs.

Table S2. Raw data of unspiked runs for other twelve geological reference materials relative to NIST SRM 915a.

Table S3. Raw data of double-spiked runs for NIST SRM 915a, NIST SRM 915b and Atlantic Seawater.

This material is available as part of the online article from: http://onlinelibrary.wiley.com/doi/10.1111/ggr.12153/abstract (This link will take you to the article abstract).